

## COMMUNICATION

## Spin-crossover iron (II) complex showing thermal hysteresis around room temperature with symmetry breaking and an unusually high $T(\text{LIESST})$ of 120 K.

Received 00th January 20xx,  
Accepted 00th January 20xx

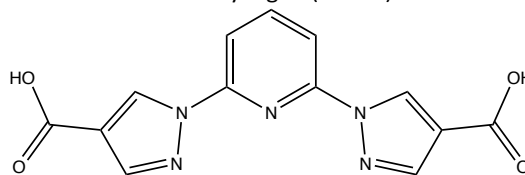
DOI: 10.1039/x0xx00000x

Víctor García-López,<sup>a</sup> Mario Palacios-Corella,<sup>a</sup> Salvador Cardona-Serra,<sup>a</sup> Miguel Clemente-León\*<sup>a</sup> and Eugenio Coronado<sup>a</sup>

**We report a Fe(II) complex based on 4',4'' carboxylic acid disubstituted dipyrazolylpyridine that shows a spin-crossover close to room temperature associated to a crystallographic phase transition and LIESST effect with a high  $T(\text{LIESST})$  of 120 K.**

Spin-crossover (SCO) complexes can be reversibly switched between two distinct states by a variety of external stimuli such as light, temperature, pressure, or electric fields.<sup>1</sup> SCO applications based on thermal effects require abrupt and hysteretic thermal SCO close to room temperature, as the bi-stability in this hysteresis loop would confer a memory effect to the system. On the other hand, the use of light permits very fast, selective and reversible spin state switching taking advantage of the Light-Induced Excited Spin State Trapping (LIESST) effect.<sup>2</sup> Since LIESST compounds are photo-activated molecular switches, there is great interest in finding compounds operating at high temperature.<sup>3</sup> From the theoretical part, mean-field theory predicts an inverse relationship between the thermodynamic thermal SCO temperature  $T_{1/2}$  ( $T_{1/2}$  = temperature of 50 % high-spin (HS) to low-spin (LS) conversion) and the lifetime of the photoinduced metastable state. Due to this, with the exception of a few Fe-Co Prussian blue analogues,<sup>4</sup> there are no reports of Fe coordination compounds combining thermal SCO around room temperature and photo-induced SCO at temperatures above 100 K. Thus, in Fe(II) complexes an empirical linear dependence between  $T(\text{LIESST})$ , which is the relaxation temperature above which the metastable photoinduced state is erased, and  $T_{1/2}$  has been proposed by Létard et al., in which  $T(\text{LIESST}) = T_0 - 0.3 T_{1/2}$ .  $T_0$  is the initial value of the linear function, which could be related to the denticity and rigidity of the ligand.<sup>5-7</sup> Although important deviations from this law have been found, it is a useful tool to predict  $T(\text{LIESST})$  of many SCO

compounds.<sup>2</sup> For instance,  $T(\text{LIESST})$  of the well-known family of bis-chelated iron(II) complexes of the tridentate 2,6-bis(pyrazol-1-yl)pyridine (bpp)<sup>3,8</sup> usually show good agreement with this linear function with  $T_0 = 150$  K. This means that the highest values of  $T(\text{LIESST})$  for this family of compounds (~100 K) correspond in all cases to  $T_{1/2}$  values below 200 K, which are far from room temperature.<sup>5-10</sup> In previous works, we functionalized bpp with carboxylic acid in different positions of the pyridine ring to study the effect of this functional group in the SCO properties of the complex and as a way for depositing this complex on surfaces or forming extended networks through coordination with the carboxylic acid groups. This strategy yielded homoleptic and heteroleptic complexes, which showed abrupt thermal SCO with hysteresis and LIESST effect, and a polynuclear complex.<sup>11-15</sup> Here, we have extended this approach to a new bpp derivative functionalized with carboxylic acid groups in the 4-positions of the two pyrazolyl groups of bpp (bpCOOH<sub>2p</sub>, see scheme 1). This ligand has afforded the compound  $[\text{Fe}^{\text{II}}(\text{bpCOOH}_2\text{p})_2](\text{ClO}_4)_2 \cdot 3.5\text{Me}_2\text{CO}$  (**1**), which shows an abrupt thermal SCO around room temperature and a photoinduced SCO with an unusually high  $T(\text{LIESST})$  of 120 K.



**Scheme 1.** Molecular structure of bpCOOH<sub>2p</sub>.

BpCOOH<sub>2p</sub> was prepared by saponification of the 2,6-di[4-(ethylcarboxy)pyrazol-1-yl]pyridine ester precursor.<sup>16</sup> Slow diffusion of diethyl ether on the solution of  $\text{Fe}(\text{ClO}_4)_2 \cdot x\text{H}_2\text{O}$  and bpCOOH<sub>2p</sub> in a 1:2 molar ratio in acetone yielded crystals of **1** after a few days (see ESI† for details).

The temperature dependence of molar magnetic susceptibility times temperature ( $\chi_{\text{M}}T$ ) of **1** below 270 K measured in contact with the mother liquor shows a value close to 0, typical of diamagnetic LS state ( $S=0$ ) (see Fig. 1). At higher temperatures,  $\chi_{\text{M}}T$  presents a sharp increase to a value of  $1.6 \text{ cm}^3 \cdot \text{K} \cdot \text{mol}^{-1}$  at

<sup>a</sup> Instituto de Ciencia Molecular (ICMol), Universidad de Valencia, Catedrático José Beltrán 2, 46100 Burjassot, Spain.

<sup>†</sup> Electronic Supplementary Information (ESI) available: Experimental procedures and characterization, crystallographic figures, powder diffraction data, magnetic and photomagnetic properties. For ESI and crystallographic data in CIF or other electronic format see DOI: 10.1039/x0xx00000x

300 K, consistent with a LS to HS conversion close to 50 %. A thermal hysteresis width ( $\Delta T$ ) of 13 K is observed in heating and cooling modes ( $T_{\uparrow} = 292$  K and  $T_{\downarrow} = 279$  K) at a scan rate of  $0.5$  K  $\text{min}^{-1}$ . Abrupt thermal hysteretic spin transitions with  $\Delta T = 1$ -4 K are common in bpp iron(II) complexes with a particular packing motif, the so-called "terpyridine embrace" one.<sup>3,8</sup> However, there are very few examples with wider thermal hysteresis. They are associated to compounds with distorted octahedral coordination in the HS state, crystallographic phase transitions ( $\Delta T = 18$  K<sup>9</sup>) and/or lattice solvent molecules ( $\Delta T = 35$ <sup>17</sup> and  $\sim 100$  K<sup>18</sup>).

The hysteretic spin transition was confirmed by differential scanning calorimetry (DSC) measurements in crystals protected with an oil. (Fig. S1 in the ESI<sup>†</sup> and associated text). Thus, an exothermic peak at 286 K upon cooling and an endothermic peak at 297 K in the heating mode were observed. The average enthalpy and entropy changes associated with these peaks,  $\Delta H = 17.0$  kJ  $\text{mol}^{-1}$  and  $\Delta S = 60.0$  J  $\text{K}^{-1}$   $\text{mol}^{-1}$ , are typical values for iron(II) SCO solids.<sup>19</sup> These values are similar to the ones found for other iron(II) bpp complexes,<sup>9,20</sup> although they are relatively high if we consider that only half of the Fe(II) centers undergoes a spin transition.

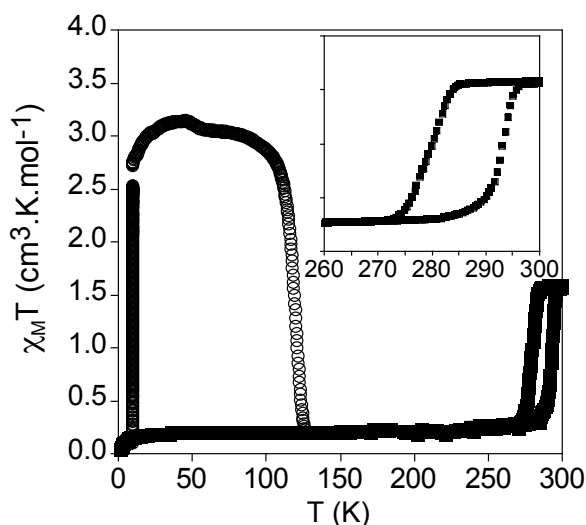


**Fig. 1** Thermal dependence of  $\chi_M T$  of **1**. Full squares: data recorded without irradiation; empty circles: data recorded after irradiation at 10 K.

$\chi_M T$  of dried crystals of **1** changes drastically. Thus, it increases to a value of  $3.6$   $\text{cm}^3 \cdot \text{K} \cdot \text{mol}^{-1}$  after heating to 400 K corresponding to 100 % HS state. This value remains almost constant with a decrease below 30 K due to zero-field-splitting of HS Fe(II) (Fig. S2 in the ESI and associated text<sup>†</sup>). This suggests that desolvation leads to irreversible structural changes that stabilize the HS state as confirmed by powder X-ray diffraction (PXRD) data (see Fig. S3 in the ESI<sup>†</sup>).

Single crystal X-ray diffraction experiments from 120 to 300 K show that this thermal SCO is related to a symmetry breaking phase-transition around 280 K. Thus, the unit cell changes reversibly above this temperature from monoclinic to triclinic

space groups (see Table S1 in the ESI<sup>†</sup>). Structure at 120 K was solved in the monoclinic space group  $P2_1/c$  showing a single molecule of  $[\text{Fe}(\text{bpCOOH}_2\text{p})_2]^{2+}$  in the asymmetric unit with typical LS Fe-N bond lengths (1.898(2)-1.977(2) Å). Above 280 K, the cell parameters  $\alpha$  and  $\gamma$  deviate significantly from  $90^\circ$  and the symmetry changes to triclinic,  $P-1$ . As a result of this, the structure at 300 K shows two molecules of  $[\text{Fe}(\text{bpCOOH}_2\text{p})_2]^{2+}$  in the asymmetric unit (with iron labelled Fe1 and Fe2) with different spin states as shown by Fe-N bond lengths (1.901(4)-1.981(5) Å for Fe1 and 2.127(4)-2.180(5) Å for Fe2). Therefore, crystal structures at 120 and 300 K and magnetic measurements indicate that there is a SCO of half of the iron(II) complexes accompanying the structural phase transition. This has been confirmed by variable temperature PRXD patterns (Figs. S3 to S5 in the ESI<sup>†</sup> and associated text).

Crystallographic symmetry breaking during SCO is a well-known phenomenon, which often leads to an intermediate crystal phase of lower symmetry containing a mixture of HS and LS molecules.<sup>21-24</sup> This mixed spin-state phase is usually retained over a temperature range. At lower or higher temperatures, it exhibits phase changes to the fully LS or HS states, respectively, with space groups of higher symmetry.<sup>21,22,25</sup> This re-entrant behavior of the intermediate phase could not be observed in **1** probably due to the irreversible loss of crystallinity caused by the removal of solvent molecules (Fig. S3 in the ESI<sup>†</sup>). DSC measurements (Fig. S1 in the ESI<sup>†</sup>) protecting the crystals with an oil show that this LS-HS phase is stable up to 320 K.

The iron(II) ion of the complex is coordinated by two tridentate bpCOOH<sub>2</sub>p ligands with a distorted octahedral geometry, which has been evaluated using  $\Sigma$  and  $\Theta$  parameters ( $\Sigma = 88.1(2)^\circ$  and  $\Theta = 278.5(1)^\circ$  at 120 K and  $\Sigma = 90.4(1)^\circ$  and  $\Theta = 282.9(2)^\circ$  for Fe1 and  $\Sigma = 152.7(2)^\circ$  and  $\Theta = 495.9(2)^\circ$  for Fe2 at 300 K).<sup>26,27</sup> These values are similar to those obtained in other bpp complexes with hysteretic spin transitions.<sup>9</sup> Another remarkable aspect is that the HS complexes exhibit a strong Jahn-Teller distortion. Thus, trans-N(pyridyl)-Fe-N(pyridyl) angles ( $\phi$ ) are  $175.70(11)^\circ$  at 120 K and  $174.80(18)^\circ$  (Fe1) and  $167.93(17)^\circ$  (Fe2) at 300 K, whereas dihedral angles between the least squares planes of the two ligands ( $\theta$ ) are  $80.2^\circ$  at 120K and  $79.4^\circ$  (Fe1) and  $77.7^\circ$  (Fe2) at 300 K. HS complexes deviating more strongly from the ideal values of  $\theta$  and  $\phi$  ( $90^\circ$  and  $180^\circ$ , respectively) are less likely to transform to their LS state upon cooling.<sup>28</sup> Indeed, most of the SCO active bpp-based compounds exhibited Jahn-Teller distortion parameters with  $\phi \geq 172^\circ$  and  $\theta \geq 76^\circ$ . However, several examples of active SCO ones with parameters outside this range have been reported recently exhibiting hysteretic spin transitions.<sup>9,18,29</sup> This seems to be the case in **1**, with a low  $\phi$  value of  $167.93^\circ$ .

The bpCOOH<sub>2</sub>p ligands form hydrogen bonds with one acetone molecule and one  $\text{ClO}_4^-$  (see Fig. S6 in the ESI<sup>†</sup>). This prevents formation of hydrogen-bonded chains of complexes as in other iron(II) complexes of bpp functionalized with carboxylic acid.<sup>11,13</sup> At 120 K, neighboring  $[\text{Fe}(\text{bpCOOH}_2\text{p})_2]^{2+}$  cations present  $\pi \cdots \pi$  interactions between the pyrazolyl rings and several short contacts involving the CO groups. This gives rise to chains of complexes along the  $c$  axis (see Fig. S7 in the ESI<sup>†</sup>).

At 300 K, there are two types of chains, which now run along the *a* axis. Chains of LS  $[\text{Fe}(\text{bpCOOH}_2\text{p})_2]^{2+}$  cations with Fe1 present similar interactions to those at 120 K (see Fig. S7 in the ESI<sup>†</sup>). In contrast to this, the HS  $[\text{Fe}(\text{bpCOOH}_2\text{p})_2]^{2+}$  cations with Fe2 form chains with a smaller number of intermolecular interactions. These chains are linked at 120 K through several contacts leading to a double layer of complexes in the *bc* plane (see Fig. 2). Similar features in the *ab* plane are found in the structure at 300 K but in this case, complexes with Fe1 and Fe2 belonging to different chains present stronger intermolecular interactions (see Fig. S8 in the ESI<sup>†</sup>). In summary, the structures at 120 and 300 K present similar packing motifs with important differences: 1) The structure at 300 K shows weaker intrachain contacts for the HS complexes and stronger interchain contacts between HS and LS ones; 2)  $\text{ClO}_4^-$  and acetone molecules are disordered at 300 K but not at 120 K.

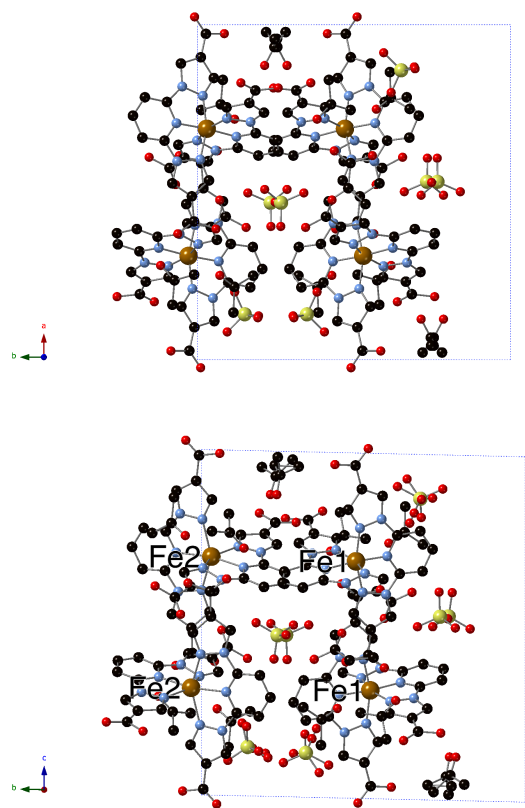


**Fig. 2** Projection of the structure of **1** in the *ab* plane at 120 K (top) and in the *bc* plane at 300 K (bottom). Fe (orange) C (black), N (blue), O (red), Cl (yellow).

The LS to HS photoconversion was investigated by irradiation of crystals of **1** protected with an oil at 10 K with red and green light. A drastic increase of the magnetic signal was observed after irradiation at the two wavelengths. Red light led to faster increase of the signal but saturation was only reached after more than 8 hours. This long irradiation time could suggest some structural reorganization of the compound. After this time, irradiation was switched off and the temperature was then increased at a rate of  $0.3 \text{ K min}^{-1}$ . The  $\chi_{\text{MT}}$  value after irradiation is higher than the value recorded in the dark at temperatures below 120 K (see empty circles in Fig. 1). The fraction of Fe(II) photoconverted after irradiation is calculated

to be close to 100 % in contrary to the LS-HS state reached after heating above 280 K. The abrupt decrease of the LIESST curve above 110 K confirms that an intermediate HS-LS state is not reached after photoexcitation. The  $T(\text{LIESST})$ , defined as the minimum of the derivative of  $\chi_{\text{MT}}$  with temperature after irradiation, is 120 K (see Fig. S9 in the ESI<sup>†</sup>). Notice that **1** represents one of the few molecular compounds with  $T(\text{LIESST})$  well above  $100 \text{ K}$ <sup>5,9,10,30</sup> but, in contrast to these examples, **1** exhibits a  $T_{1/2}$  near room temperature. Therefore,  $T_{1/2}$  and  $T(\text{LIESST})$  values deviates clearly from the linear relationship found for other iron(II) bpp complexes.

The relaxation from the photoinduced HS state to the LS state has been investigated from 105 to 115 K close to the  $T(\text{LIESST})$ . Time dependence of the HS fraction could be fitted to a sigmoidal decay typically found in cooperative systems with a self-accelerated behaviour. Therefore, the measurements have been fitted using the mean-field macroscopic model developed by Hauser (see Fig. S10 in the ESI<sup>†</sup> and associated text).<sup>31,32</sup> Parameters obtained from these fittings are in the same range as those of other bpp complexes ( $E_{\text{a}} = 2385 \text{ cm}^{-1}$ ,  $k_{\infty} = 1.2 \cdot 10^{11} \text{ s}^{-1}$ ,  $E_{\text{a}}^* = 4.08 \text{ cm}^{-1}$  and  $k_0 \leq 9.07 \cdot 10^{-5} \text{ s}^{-1}$  where  $E_{\text{a}}$  is the apparent activation energy,  $k_{\infty}$  is the apparent preexponential factor,  $E_{\text{a}}^*$  is the additional activation energy resulting from cooperativity and  $k_0$  is the upper limit of the tunnelling rate constant).<sup>9,33-36</sup>

The thermally-induced excited spin-state trapping (TIESST) was not observed after cooling the sample from room temperature to 10 K in a few seconds. This is not unexpected as this effect is usually found in compounds with  $T_{1/2}$  below  $200 \text{ K}$ .<sup>9</sup>

Finally, we have explored the deposition on  $\text{SiO}_2$  surfaces and the preparation of coordination polymers. Preliminary results indicate that these complexes decompose on  $\text{SiO}_2$  surfaces as observed for other bpp complexes functionalized with carboxylic acid.<sup>15</sup> On the other hand, the coordination polymer  $[\text{Fe}^{\text{II}}(\text{bpCOO}(\text{COOH})\text{p})(\text{bpCOOH}_2\text{p})\text{Fe}^{\text{II}}(\text{bpCOOH}_2\text{p})(\text{ClO}_4)_2 \cdot \text{H}_2\text{O} \cdot 1.5\text{Me}_2\text{CO}$  (**2**) was obtained in the synthesis of **1** if the diffusion tubes were left in air for longer times (see Figs. S12 and S13 in the ESI<sup>†</sup> and associated text).

Our results indicate that in **1**, the combination of a rigid bpp ligand, which leads to distorted HS geometries, and carboxylic acid groups favouring the presence of solvent molecules in the structure, which enable enough free volume for the distorted HS molecules to switch to the undistorted LS state, could be crucial factors to explain the abrupt thermal SCO with hysteresis of **1**. This agrees with that observed in other bpp-based compounds<sup>9,28</sup> and with the gradual SCO of **2**, which contains the same ligand but with a less distorted octahedral geometry and a less flexible extended lattice. In addition to this, **1** presents an unexpectedly long-lived photo-induced state for such thermal spin transition. Large trigonal distortions as that of **1** have been used to explain stabilization of the HS state and increase of  $T(\text{LIESST})$ .<sup>2,9</sup> However, this would cause at the same time a decrease of  $T_{1/2}$ , which is not observed in **1**, in contrast to bpp-based compounds with HS distorted structures.<sup>3,9,10,28</sup> This suggests that besides the distortion of the octahedral geometry, a photoinduced structural change could be at the origin of the unexpected

behavior of **1**. Indeed, this has been observed in  $[\text{Fe}(\text{L})_2](\text{BF}_4)_2 \cdot \text{S}$  ( $\text{L} = 4\text{-}(\text{Isopropylsulfanyl})\text{-}2,6\text{-di}(\text{pyrazol-}1\text{-yl})\text{pyridine}$ ). This compound presents a  $T(\text{LIESST})$  lower than the expected one, which is attributed to a photo-induced crystallographic phase transition.<sup>10</sup> In our case, we would have the opposite behavior. Photocrystallographic studies are needed to support this hypothesis. These measurements are in progress and will be reported in due course. Finally, **2** shows the expected  $T(\text{LIESST})$  and  $T_{1/2}$  values (see ESI<sup>†</sup>). This indicates that the unexpected behavior of **1** is not general for bpCOOHp Fe(II) complexes. In summary, **1** combines two unexpected properties: SCO around room temperature and a long-lived photoinduced HS state at extraordinary high temperatures, which are associated to a specific crystal structure very sensitive to the presence of solvent molecules. The complete understanding of the SCO behaviour of **1** could be a step towards the rational design of new SCO complexes with improved properties. Financial support from the EU (ERC Advanced Grant MOL-2D 788222), the Spanish MINECO and FEDER funds (MAT-2017-89993-R, CTQ2017-89528-P and Unidad de Excelencia María de Maeztu MDM-2015-0538) and the Generalitat Valenciana (PROMETEO program) is gratefully acknowledged. SCS thanks the Spanish MINECO for a Juan de la Cierva – Incorporación grant. We all thank A. Soriano-Portillo, J. M. Martínez-Agudo and G. Agustí for PXRD and magnetic measurements.

### Conflicts of interest

There are no conflicts to declare.

### Notes and references

- (a) Eds. P. Gülich and H.A. Goodwin, *Spin Crossover in Transition Metal Compounds*, *Topics in Current Chemistry*, Springer Verlag, Berlin-Heidelberg-New York, 2004, vols. 233-235; (b) Ed. M. A. Halcrow, *Spin-Crossover Materials: Properties and Applications*, John Wiley & Sons, Chichester, UK, 2013.
- G. Chastanet, C. Desplanches, C. Baldé, P. Rosa, M. Marchivie and P. Guionneau, *Chem. Sq.*, 2018, **2**, 2.
- M. A. Halcrow, *Coord. Chem. Rev.*, 2009, **253**, 2493.
- N. Shimamoto, S. I. Ohkoshi, O. Sato and K. Hashimoto, *Inorg. Chem.*, 2002, **41**, 678.
- S. Marcén, L. Lecren, L. Capes, H. A. Goodwin and J. F. Létard, *Chem. Phys. Lett.*, 2002, **358**, 87.
- V. A. Money, J. Sánchez-Costa, S. Marcén, G. Chastanet, J. Elhaik, M. A. Halcrow, J. A. K. Howard and J. F. Létard, *Chem. Phys. Lett.*, 2004, **391**, 273.
- J. F. Létard, P. Guionneau, O. Nguyen, J. Costa, S. Marcén, G. Chastanet, M. Marchivie and L. Goux-Capes, *Chem. Eur. J.*, 2005, **11**, 4582.
- (a) M. A. Halcrow, *Coord. Chem. Rev.*, 2005, **249**, 2880; (b) J. Olguín and S. Brooker, *Coord. Chem. Rev.*, 2011, **255**, 203; (c) M. A. Halcrow, *New J. Chem.*, 2014, **38**, 1868; (d) L. J. Kershaw Cook, R. Mohammed, G. Sherborne, T. D. Roberts, S. Alvarez and M. A. Halcrow, *Coord. Chem. Rev.*, 2015, **289–290**, 2.
- L. J. Kershaw Cook, F. L. Thorp-Greenwood, T. P. Comyn, O. Cespedes, G. Chastanet and M. A. Halcrow, *Inorg. Chem.*, 2015, **54**, 6319.
- R. Kulmaczewski, E. Trzop, L. J. Kershaw Cook, E. Collet, G. Chastanet and M. A. Halcrow, *Chem. Commun.*, 2017, **53**, 13268.
- A. Abhervé, M. Clemente-León, E. Coronado, C. J. Gómez-García and M. López-Jordà, *Dalton Trans.*, 2014, **43**, 9406.
- A. Abhervé, M. J. Recio-Carretero, M. López-Jordà, J. M. Clemente-Juan, J. Canet-Ferrer, A. Cantarero, M. Clemente-León and E. Coronado, *Inorg. Chem.*, 2016, **55**, 9361.
- V. García-López, M. Palacios-Corella, A. Abhervé, I. Pellicer-Carreño, C. Desplanches, M. Clemente-León and E. Coronado, *Dalton Trans.*, 2018, **47**, 16958.
- V. García-López, M. Palacios-Corella, M. Clemente-León and E. Coronado, *Polyhedron*, 2019, **170**, 95.
- V. García-López, M. Palacios-Corella, V. Gironés-Pérez, C. Bartual-Murgui, J. A. Real, E. Pellegrin, J. Herrero-Martín, G. Aromí, M. Clemente-León and E. Coronado, submitted.
- R. Pritchard, C. A. Kilner, S. A. Barrett and M. A. Halcrow, *Inorganica Chimica Acta*, 2009, **362**, 4365.
- H. Douib, L. Cornet, J. Flores González, E. Trzop, V. Dorcet, A. Gouasmia, L. Ouahab, O. Cadot and F. Pointillart, *Eur. J. Inorg. Chem.* 2018, **2018**, 4452.
- K. Senthil Kumar, B. Heinrich, S. Vela, E. Moreno-Pineda, C. Bailly and M. Ruben, *Dalton Trans.*, 2019, **48**, 3825-3830.
- S. Rat, J. Sánchez Costa, S. Bedoui, W. Nicolazzi, G. Molnár, L. Salmon and A. Bousseksou, *Pure Appl. Chem.*, 2015, **87(3)**, 261.
- A. Abhervé, M. Clemente-León, E. Coronado, C. J. Gómez-García and M. López-Jordà, *Dalton Trans.*, 2014, **43**, 9406.
- M. Shatruk, H. Phan, B. A. Christostomo and A. Suleimenova, *Coord. Chem. Rev.*, 2015, **289-290**, 62.
- N. Ortega-Villar, M. C. Muñoz and J. A. Real, *Magnetochemistry*, 2016, **2**, 16.
- W. Phonsri, C. G. Davies, G. N. L. Jameson, B. Moubaraki, J. S. Ward, P. E. Kruger, G. Chastanet and K. S. Murray, *Chem. Commun.*, 2017, **53**, 1374.
- H. Hang, B. Fei, X. Q. Chen, M. L. Tong, V. Ksenofontov, I. A. Gural'skiy and X. Bao, *J. Mater. Chem., C* 2018, **6**, 3352.
- I. Capel Berdiell, R. Kulmaczewski, O. Cespedes and M. A. Halcrow, *Chem. Eur. J.*, 2018, **24**, 5055.
- M. Marchivie, P. Guionneau, J. F. Létard and D. Chasseau, *Acta Cryst.*, 2003, **B59**, 479.
- $\Sigma = \sum_{i=1}^{12} |90 - \alpha_i|$ , where  $\alpha_i$  are the 12 cis-N-Fe-N angles around the iron atom, and  $\Theta = \sum_{j=1}^{24} |60 - \theta_j|$ , where  $\theta_j$  are the 24 unique N-Fe-N angles around the iron atom.
- I. Capel Berdiell, R. Kulmaczewski, O. Cespedes and M. A. Halcrow, *Chem. Eur. J.*, 2018, **24**, 5055.
- L. J. Kershaw Cook, R. Kulmaczewski, O. Cespedes and M. A. Halcrow, *Chem. Eur. J.*, 2016, **22**, 1789.
- J. Sánchez Costa, C. Baldé, C. Carbonera, D. Denux, A. Wattiaux, C. Desplanches, J. P. Ader, P. Gülich and J. F. Létard, *Inorg. Chem.*, 2007, **46**, 4114.
- A. Hauser, *Chem. Phys. Lett.*, 1992, 192, 65.
- A. Hauser, J. Jectic, H. Romstedt, R. Hinek and H. Spiering, *Coord. Chem. Rev.*, 1999, **190-192**, 471.
- C. Carbonera, J. Sánchez Costa, V. A. Money, J. Elhaik, J. A. K. Howard, M. A. Halcrow and J. F. Létard, *Dalton Trans.*, 2006, 3058.
- V. A. Money, C. Carbonera, J. Elhaik, M. A. Halcrow, J. A. K. Howard, and J. F. Létard, *Chem. Eur. J.*, 2007, **13**, 5503.
- R. Pritchard, H. Lazar, S. A. Barrett, C. A. Kilner, S. Asthana, C. Carbonera, J. F. Létard and M. A. Halcrow, *Dalton Trans.*, 2009, 6656.
- C. Baldé, C. Desplanches, F. Le Gac, P. Guionneau and J. F. Létard, *Dalton Trans.*, 2014, **43**, 7820.